Methane conversion to synthesis gas by partial oxidation and CO_2 reforming over supported platinum catalysts

Mariana M.V.M. Souza[a] and Martin Schmal[a,b,*]

[a]*NUCAT/PEQ/COPPE, Universidade Federal do Rio de Janeiro, C.P. 68502, 21945-970, Rio de Janeiro, Brazil*
[b]*Escola de Química, Universidade Federal do Rio de Janeiro, C.P. 68542, 21940-900, Rio de Janeiro, Brazil*

Received 7 May 2003; accepted 14 August 2003

Partial oxidation of methane and reforming of methane with CO_2 were carried out with Pt/Al_2O_3, $PtZrO_2$ and Pt/CeO_2 catalysts, in the temperature range of 350–900 °C. For partial oxidation, the catalysts showed similar stabilities, with the PtZr slightly more active. The reaction occurs in two simultaneous stages: total combustion of methane and reforming of the unconverted methane with steam and CO_2, with the O_2 conversion of 100% over the whole temperature range. For reforming with CO_2, the catalysts presented similar activities, but with distinct deactivation rates: while the PtAl deactivates very fast at 800 °C, due to deposition of inactive carbon, the PtZr and PtCe catalysts offer higher resistance to coke formation, due to the metal-support interactions and the higher mobility of oxygen in the oxide lattice.

KEY WORDS: methane; syngas; partial oxidation; reforming; platinum; catalysts.

1. Introduction

There has been substantial interest in recent years in alternative routes for conversion of natural gas (methane) to synthesis gas, a mixture of CO and H_2, which can be used to produce chemical products with high added values, such as hydrocarbons and oxygenated compounds. Generally, methane is converted to synthesis gas by steam reforming, but it requires a large amount of heat addition and the H_2/CO ratio obtained (about 3) is too high for fuel synthesis via Fischer–Tropsch reaction [1,2]. Moreover, steam reformers are inadequate for hydrogen generation in fuel cell electric vehicles because of their high thermal inertia for frequent start-up and shut-down operation condition [3,4].

Methane partial oxidation is an advantageous route for synthesis gas production for both economical and technical reasons: it makes the process less energy-intensive and capital cost-intensive because of its exothermic nature, and the lower H_2/CO ratio (about 2) is more favorable with respect to downstream processes such as methanol synthesis and Fischer–Tropsch synthesis of higher hydrocarbons [5–7]. In addition, a fuel processor based on partial oxidation of methane could provide a low cost and compact system, with fast start-up and capability to follow load variations, more adequate for fuel cell electric vehicles [4].

$$CH_4 + \tfrac{1}{2}O_2 \Leftrightarrow CO + 2H_2 \quad \Delta H_{298K} = -36\,\text{kJ/mol} \quad (1)$$

Reforming of methane with CO_2 is another alternative route with important advantages for some applications since the H_2/CO product ratio (about 1) is more adequate for synthesis of oxoalcohols, acetic acid and dimethyl ether [8]. It is also an environment-friendly process because it reduces CO_2 emissions, which is the main source of the greenhouse effect.

$$CH_4 + CO_2 \Leftrightarrow 2CO + 2H_2 \quad \Delta H_{298K} = 247\,\text{kJ/mol} \quad (2)$$

Although development of catalysts on the basis of nonnoble metals (e.g. Fe, Co, Ni) is of interest from the industrial point of view, numerous studies have demonstrated that noble metal catalysts exhibit better activity and suffer less carbon deposition [9–11]. There is evidence that the support has a significant effect on the overall catalytic behavior and the use of reducible oxides, like ZrO_2 and CeO_2, can result in additional process benefits when compared to irreducible oxides, such as Al_2O_3, SiO_2 or MgO [12–14]. The reducibility and oxygen transfer capacity of ZrO_2 and CeO_2 have shown to be fundamental in keeping the active-phase surface free of carbon deposits [14,15]. The role of these oxides is closely related to a bifunctional mechanism in which oxygen from the oxide lattice reacts with the carbonaceous species adsorbed on the noble metal, while the partially reduced oxide is simultaneously reoxidized by the gaseous oxidant (O_2 or CO_2). Thus, the reaction takes place basically at the metal-support interface [14–16].

The aim of this work is to investigate the role of the reducible oxides ZrO_2 and CeO_2 in the activity and stability of supported platinum catalysts for methane partial oxidation and CO_2 reforming, comparing with the catalytic behavior of Pt/Al_2O_3.

* To whom correspondence should be addressed.
E-mail: schmal@peq.coppe.ufrj.br

1011-372X/03/1100–0011/0

2. Experimental

2.1. Catalyst preparation

Al_2O_3, ZrO_2 and CeO_2 supports were prepared by calcination of γ-alumina (Engelhard Corporation Catalyst), zirconium hydroxide (MEL Chemicals) and cerium ammonium nitrate (Aldrich) at 550 °C for 2 h under flowing air.

The platinum catalysts were prepared by incipient wetness impregnation of the supports with an aqueous solution of chloroplatinic acid (H_2PtCl_6, Aldrich), followed by drying at 120 °C for 16 h and calcination in air at 550 °C for 2 h. All samples contained about 1 wt% of platinum, which was determined by atomic absorption spectrometry. The prepared catalysts are referred to as PtAl for Pt/Al_2O_3, PtZr for Pt/ZrO_2 and PtCe for Pt/CeO_2.

2.2. Catalyst characterization

H_2 and CO chemisorption analyses were obtained at room temperature using an automatic adsorption system (ASAP 2000, Micromeritics). The samples were pretreated with helium flux at 150 °C for 1 h. After reduction at 300 or 500 °C under 10% H_2/Ar flow, the samples were evacuated at 10^{-6} torr for 30 min at the reduction temperature and cooled to room temperature. Irreversible H_2 and CO uptakes were obtained from the total and reversible adsorptions isotherms taken in a pressure range of 50–350 mm Hg.

TPR apparatus and methodology are described in [17]. The samples were dehydrated at 150 °C under flowing argon before the reduction. A mixture of 1.65% hydrogen in argon flowed at 30 mL/min through the sample, raising the temperature at a heating rate of 10 °C/min up to 900 °C.

2.3. Catalyst testing

Before each catalytic test, the catalysts were dried *in situ* with flowing nitrogen at 150 °C for 30 min, following the reduction with 10% H_2/N_2 at a rate of 10 °C/min to 500 °C and remaining at this temperature for 1 h. After reduction, the catalyst was purged with N_2 for 30 min at the same temperature. The reaction was carried out in a fixed-bed flow-type quartz reactor loaded with 20 mg of catalyst, under atmospheric pressure. A thermocouple was placed on top of the catalyst bed to measure catalyst temperature. The total feed flow rate was held constant at 200 cm^3/min (WHSV = 600 000 $cm^3/h/g_{cat}$) with flowing helium. The gas compositions are listed in table 1. The activity tests were performed at different temperatures, ranging from 450 to 900 °C in steps of 50 °C that were kept for 30 min at each temperature. The loss in catalyst activity at 800 °C was monitored up to 60 h onstream. The reaction products were analyzed by on-line gas chromatograph (CHROMPACK CP9001), equipped with a Hayesep D column and a thermal conductivity detector.

Table 1
Flow rates for activity and deactivation tests (cm^3/min)

Test no.	CH_4	CO_2	O_2	He	Total
1	10	0	5	185	200
2	10	0	4	186	200
3	10	0	6	184	200
4	10	10	0	180	200

The amount of coke formed over the catalysts after deactivation tests at 800 °C was examined by thermogravimetric analysis (TGA), using a RIGAKU thermoanalyzer (model TAS 100). The samples were pretreated at 150 °C under flowing nitrogen and then heated at a rate of 10 °C/min to 800 °C in a flow of 15% O_2/N_2 (50 cm^3/min).

3. Results and discussion

3.1. Catalyst characterization

The amounts of irreversibly adsorbed H_2 and CO at room temperature after low-temperature (LTR) and high-temperature reduction (HTR) are reported in table 2. After reduction at 500 °C, the PtAl catalyst presented high H/Pt values, which can be associated with the presence of oxychlorinated platinum complexes (PtO_xCl_y), due to the specific capacity of alumina to retain chlorine ions [18,19]. After reduction at 300 °C, the H_2 and CO uptakes on this catalyst decreased

Table 2
H_2 and CO chemisorptions on platinum catalysts

Catalyst	T reduction (°C)	H_2 uptake (μmol/g_{cat})	H/Pt	CO uptake (μmol/g_{cat})	CO/Pt	CO/H_2
PtAl	300	19.0	0.74	27.3	0.53	1.4
	500	22.3	0.87	35.7	0.70	1.6
PtZr	300	14.6	0.57	57.1	1.11	3.9
	500	8.8	0.34	60.9	1.19	6.9
PtCe	300	30.8	1.21	37.5	0.74	1.2
	500	15.1	0.59	15.7	0.31	1.0

slightly as a consequence of the incomplete reduction of platinum at this temperature, as will be shown by TPR.

The lower dispersion of the PtZr catalyst might be associated with the retention of small amounts of chlorine by zirconia, creating platinum oxide species instead of PtO_xCl_y, and due to the lower specific surface area of zirconia ($62\,m^2/g$) as compared to alumina ($200\,m^2/g$). After HTR, the H_2 chemisorption on PtZr was markedly decreased compared to that on PtZr reduced at 300 °C, which suggests the migration of partially reduced zirconia onto the platinum surface (a SMSI-type state). However, the presence of ZrO_x moieties did not cause any decrease in CO chemisorption on this catalyst. The high values of the CO/H_2 ratio for the PtZr catalyst predict an interaction of CO with the Pt-ZrO_x interface, as shown by FTIR of CO in a previous paper [20].

The H/Pt value greater than 1 for the PtCe catalyst after reduction at 300 °C is typical of CeO_2-supported catalysts [21,22] and is a consequence of the high capacity of H_2 spillover from the metal to the support [23]. The decrease in the H/Pt value after the HTR may be due to partial covering of the metal by the reduced support, but this phenomenon is likely to occur with CeO_2 only after H_2 treatment above 700 °C [24]. Thus, the partial suppression of H_2 uptake after the HTR should be related to a decrease in the rate of H_2 spillover, which can be induced by the presence of a fully reduced surface. The CO/Pt value also decreases with the reduction temperature for the PtCe catalyst, although the amount of CO chemisorbed by ceria grows as the degree of ceria reduction is increased [24].

The TPR profile of the PtCe catalyst is displayed in figure 1. The experimental and theoretical H_2 uptakes are presented in table 3, assuming the reduction $Pt^{4+} \rightarrow Pt^0$. The reduction profile of PtAl (not shown) was similar to those reported in the literature [19,25]. The PtAl catalyst exhibited a maximum reduction rate at 280 °C, which has been related to the reduction of an oxychloroplatinum surface complex, such as $[Pt(OH)_xCl_y]_s$ and $[PtO_xCl_y]_s$ [18].

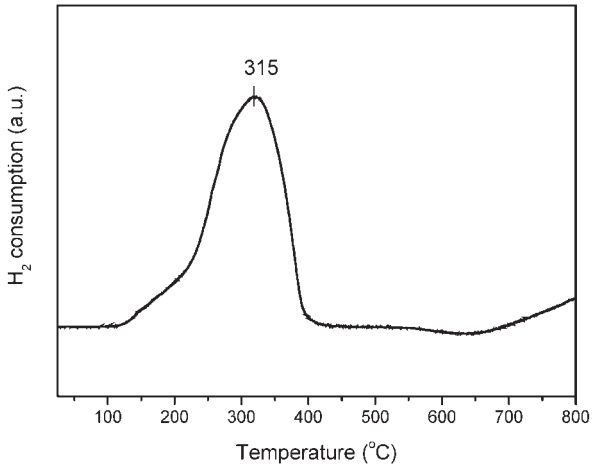

Figure 1. TPR profile for the PtCe catalyst. Conditions: 1.65%H_2/Ar, 10°C/min and GHSV = $2118\,cm^3/h/g_{cat}$.

Table 3
Temperature-programmed reduction results

Catalyst	Experimental uptakes (μmol H_2/g_{cat})	Theoretical uptakes[a] (μmol H_2/g_{cat})
PtAl	81.6	88.2
PtZr	129.1[b]	85.1
PtCe	484.8	110.0

[a]The platinum loading was quantified by atomic absorption spectrometry.
[b]Calculated using integration of the first peak only.

The TPR profile of PtZr catalyst exhibited three main peaks—at 230, 360 and 525°C, with a final stoichiometry of $ZrO_{1.98}$ [20]. The H_2 uptake corresponding to the first peak (230 °C) was higher than that needed for complete platinum reduction (table 3). As pure zirconia did not present H_2 consumption during TPR, the additional H_2 consumption by the PtZr catalyst may be associated to the reduction of zirconia at the metal interface. The other two peaks are attributed to the additional reduction of the support.

The PtCe catalyst presented a broad peak at 315 °C, with a shoulder at lower temperatures, and the H_2 uptake was more than four times higher than the theoretical one, which clearly indicates the reduction of the support. For pure CeO_2, two peaks were observed around 500 and 820 °C—the first peak corresponding to the reduction of the surface capping oxygen of ceria and the second one to the reduction of the ceria lattice [4,22]. The presence of platinum strongly modifies the features of the TPR profile, with the first peak shifted to lower temperatures. Most of the H_2 consumed in this low-temperature region can be associated to the removal of the readily available surface oxygen adjacent to the metal through a spillover mechanism, with a degree of reduction corresponding to $CeO_{1.93}$.

3.2. Partial oxidation of methane

The effect of the temperature on the CH_4 conversion for the partial oxidation reaction is displayed in figure 2. The activities of supported platinum catalysts were influenced by the nature of the support, with a better activation of the PtZr at low temperatures. PtAl was the most active catalyst over the mid-temperature range (550–650 °C), and, at higher temperatures, PtAl and PtZr exhibited activities greater than PtCe. The activity of PtAl was similar to that reported by Vernon *et al.* [9], which closely attained the thermodynamic equilibrium values. The Pt/CeO_2 prepared by Pantu and Gavalas [14] gave considerably higher methane conversion than Pt/Al_2O_3 at temperatures up to 650 °C, which was related to the reducibility of the support; above 700 °C, the activities of both catalysts were comparable. The

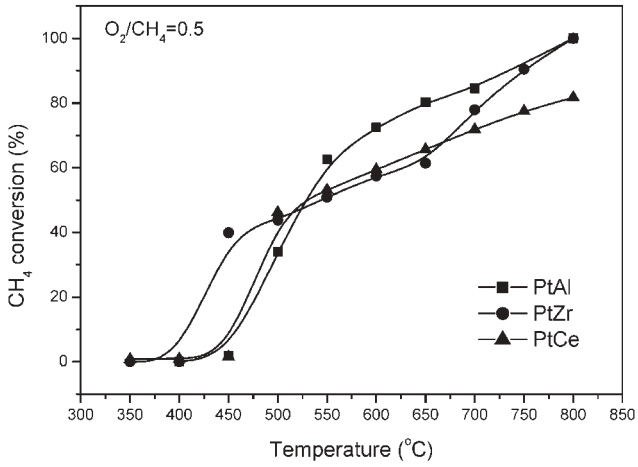

Figure 2. CH_4 conversion of platinum catalysts for partial oxidation of methane as a function of temperature (each point was taken after 30 min onstream). Conditions: test 1, table 1.

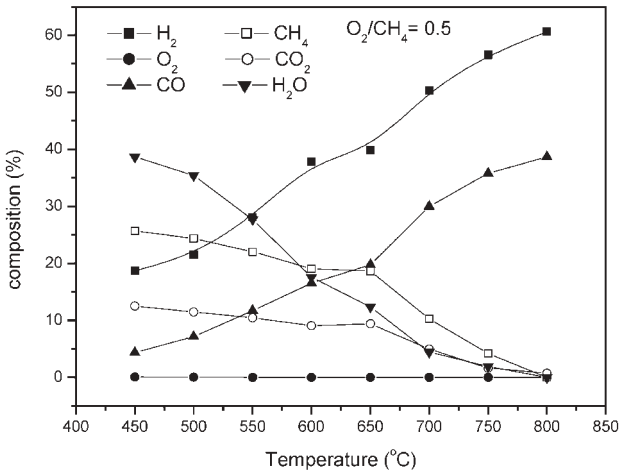

Figure 4. Composition profiles for partial oxidation of methane as a function of temperature over the PtZr catalyst. Conditions: test 1, table 1.

difference in the catalytic performance of Pt/CeO_2 may be due to the preparation method of CeO_2, which has direct influence over the morphology of the catalyst.

The H_2/CO product ratio of platinum catalysts during methane partial oxidation is shown in figure 3, as a function of temperature. At low temperatures, the H_2/CO ratio is about 3 for PtZr and PtCe catalysts and 2.2 for PtAl. As temperature rises, the H_2/CO ratio decreases up to a value of 1.5 for all catalysts. The high H_2/CO ratio at low temperatures is associated to the reforming of methane with steam produced by total combustion, which suggests that the reforming with steam is faster than reforming with CO_2.

$$CH_4 + 2O_2 \Leftrightarrow CO_2 + 2H_2O \qquad \Delta H_{298\,K} = -802\,kJ/mol \quad (3)$$

$$CH_4 + H_2O \Leftrightarrow CO + 3H_2 \qquad \Delta H_{298\,K} = 206\,kJ/mol \quad (4)$$

At higher temperatures, the H_2/CO ratio is mainly related to the partial oxidation of methane (reaction 1)

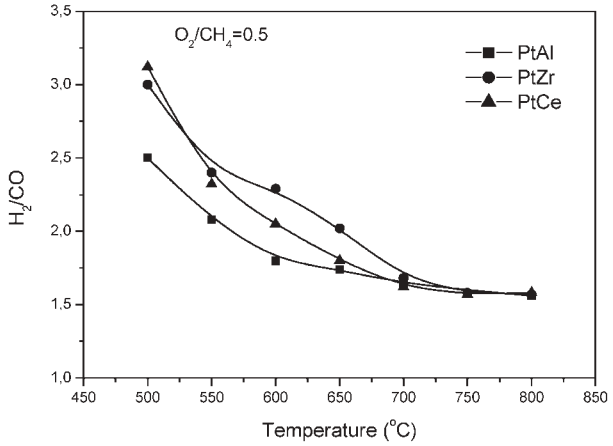

Figure 3. The H_2/CO product ratio for partial oxidation of methane as a function of temperature. Conditions: test 1, table 1.

with simultaneous water–gas shift reaction:

$$CO_2 + H_2 \Leftrightarrow CO + H_2O \qquad \Delta H_{298\,K} = 41\,kJ/mol \quad (5)$$

A two-step mechanism has been proposed for the partial oxidation of methane [26,27]. In the first step, combustion of methane takes place, producing CO_2 and H_2O; in the second step, synthesis gas is produced via CO_2 and steam reforming reactions of unreacted methane. This indirect mechanism is clearly evidenced by the composition profiles shown in figure 4 for the PtZr catalyst. The O_2 conversion is 100% over the whole temperature range. The production of steam and CO_2 decreases rapidly with temperature increase owing to the exothermic nature of total combustion (reaction 3). The high production rates of H_2 and CO at temperatures as low as 450 °C can be attributed to the heat released by combustion, since at these temperatures, the catalytic activities are very low for the reforming of methane with CO_2 or steam in the absence of oxygen.

The effect of O_2/CH_4 feed ratio on the CH_4 conversion at various temperatures between 300 and 800 °C for the PtZr catalyst can be seen in figure 5. Increasing the O_2/CH_4 ratio from 0.4 to 0.6 resulted in a higher methane conversion of about 25% over the temperature range of 450–600 °C, with an increase in the CO_2 and H_2O production due to total combustion of methane. Under oxygen-deficient condition (O_2/CH_4 ratio of 0.4), only a small amount of CO_2 and H_2O is produced, resulting in high H_2 and CO selectivities. Under this low feed ratio, there was a decrease in CH_4 conversion at higher temperatures, which can be related to the catalyst deactivation. Similar behavior was observed for PtAl and PtCe catalysts.

3.3. CO_2 reforming

The comparison of catalyst activities for CO_2 reforming of methane is displayed in figures 6 and 7,

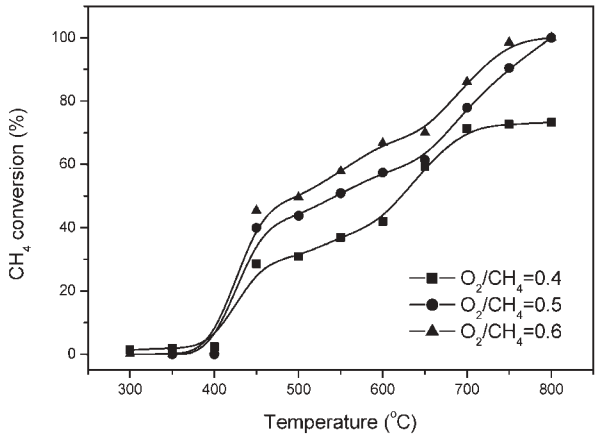

Figure 5. CH_4 conversion versus temperature for partial oxidation of methane using different gas compositions over the PtZr catalyst. Conditions: tests 1, 2 and 3, table 1.

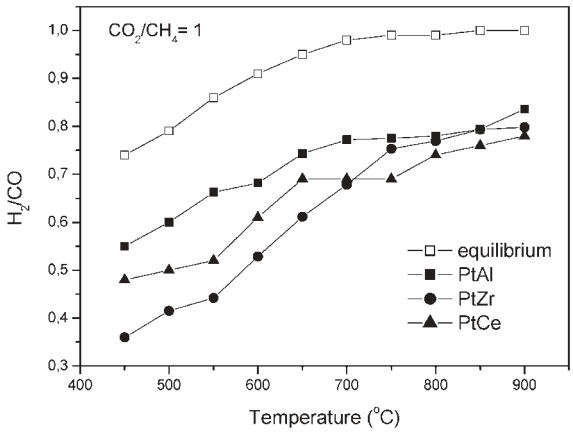

Figure 7. H_2/CO product ratio for CO_2 reforming of methane as a function of temperature. Conditions: test 4, table 1.

in terms of CH_4 conversion and H_2/CO product ratio respectively. All three catalysts exhibited similar activities, with a maximum difference of about 15% in CH_4 conversion. The PtZr presented lower activity between 600 and 700 °C, but it is the most active at temperatures higher than 750 °C. The higher activity of PtZr at high temperatures can be associated to the formation of Pt-Zr^{n+} interfacial sites, which are able to promote CO_2 activation, as demonstrated by FTIR measurements in a previous paper [20].

Wang and Ruckenstein previously reported that rhodium supported on reducible oxides had much lower activity and selectivity than rhodium on irreducible oxides for CO_2 reforming [28] and partial oxidation of methane [29]. The difference was attributed to the partial coverage of rhodium sites by the reducible oxides and the high total combustion activity of the reducible oxides. The activity sequence was the opposite to that of reducibility, i.e., the initial activity of the reducible oxides decreased with the increase in their reducibility, with CeO_2 much more reducible than ZrO_2. It should be noticed, however, that the reducible oxides used in their study had very low surface areas (less than $5\,m^2/g$). Moreover, the rhodium surface areas of the reducible oxides were approximately one order of magnitude lower than those of the irreducible oxides. Thus, the lower activity of rhodium supported on the reducible oxides could be due to their lower support and metal surface areas.

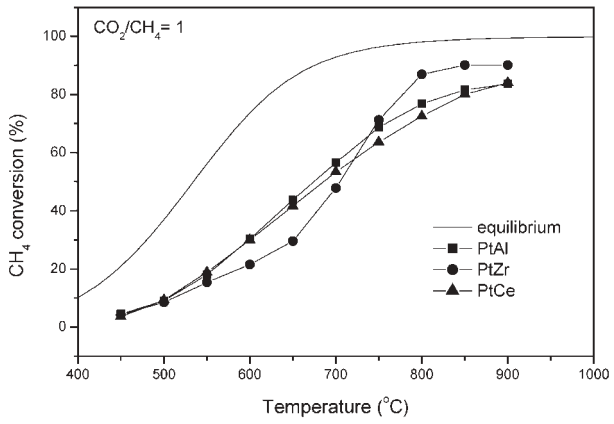

Figure 6. CH_4 conversion of platinum catalysts for CO_2 reforming of methane as a function of temperature (each point was taken after 30 min onstream). Conditions: test 4, table 1.

The methane conversion was always lower than CO_2 conversion, although they were presented in the feed in a 1 : 1 ratio, and the H_2/CO product ratio was always lower than 1 (figure 7), which is ascribed to the simultaneous occurrence of the reverse water-gas shift reaction (reaction 5). Wolf *et al.* [30] showed that the experimental values of CO and H_2 selectivities approach the values determined by the water-gas shift equilibrium already at low methane conversion and mainly at temperatures below 700 °C. At higher temperatures, the influence of the WGS reaction is lower and the H_2/CO ratio tends to 1. At low temperatures, the H_2/CO product ratio was significantly lower for the PtZr catalyst, because of the small rate of H_2 formation on this catalyst, while the CO production is kept constant. The low H_2 formation by this catalyst can be related to the reaction with carbonaceous deposits formed during the first 30 min onstream, as shown by TPSR [31].

3.4. Deactivation studies

The comparison of catalyst stabilities for partial oxidation of methane at 800 °C is shown in figure 8. The catalysts exhibited similar initial activities, with the PtCe slightly less active, and the deactivation rates were also very close: 0.21%/h for PtAl, 0.18%/h for PtZr and 0.23%/h for PtCe, during 29 h onstream. The deactivation is related to the deposition of inactive carbon over the active surface, and the amount of coke on these catalysts was quantified by thermogravimetric analysis carried out in an oxygen-containing atmosphere. The amount of coke was relatively small for all catalysts

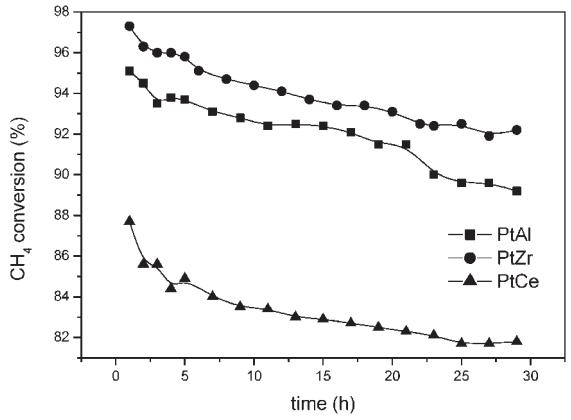

Figure 8. CH_4 conversion as a function of time onstream at 800 °C for partial oxidation of methane. Conditions: test 1, table 1.

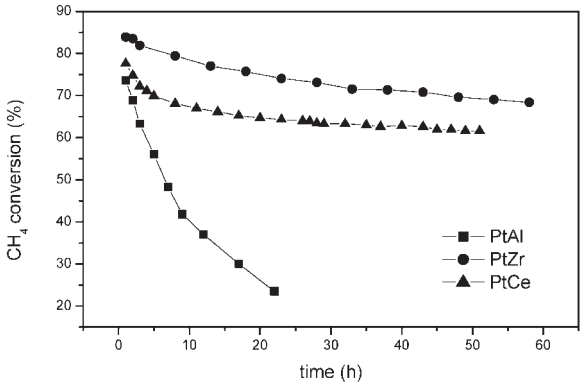

Figure 9. CH_4 conversion as a function of time onstream at 800 °C for CO_2 reforming of methane. Conditions: test 4, table 1.

(0.6–0.8 mg coke/h/g_{cat}). Thus, the catalysts supported on reducible oxides exhibited stabilities similar to that of PtAl, not showing any promotion effect due to the oxygen storage capacity of the oxides or the oxygen mobility of the oxide lattice.

The support plays a major role on the stability of the catalysts for the CO_2 reforming of methane, as shown in figure 9. Although all catalysts exhibit similar initial activities, the stability behavior differs completely with time onstream. The PtAl deactivated very fast during 22 h onstream, with a deactivation rate of about 4.0%/h, while the PtZr and PtCe remained stable up to 60 h of reaction, with deactivation rates of only 0.31 and 0.24%/h respectively. The stable behavior of PtZr and PtCe is associated with the observation of little coke formation during the reaction (0.8–0.9 mg coke/g_{cat}/h). On the other hand, TGA experiment showed a weight loss of about 12% on treating the PtAl catalyst in oxygen, indicating a significant amount of carbon deposition during 22 h onstream (approximately 5.7 mg coke/g_{cat}/h) [20].

The deposition of inactive carbon during methane reforming can be originated from either methane decomposition (reaction 6) or CO disproportionation (Boudouard reaction 7), which are thermodynamically favorable below 900 °C [32,33]:

$$CH_4 \Leftrightarrow C + 2H_2 \qquad \Delta H_{298K} = 75\,\text{kJ/mol} \qquad (6)$$

$$2CO \Leftrightarrow C + CO_2 \qquad \Delta H_{298K} = -172\,\text{kJ/mol} \qquad (7)$$

Thermodynamic calculations showed that the extent of carbon deposition during reforming decreases at higher reaction temperatures, in agreement with several experimental observations [2,12,34]. These results suggest that CO disproportionation is the main contributor to carbon deposition because it is exothermic and the equilibrium constant decreases with increasing temperature.

The higher stability of the Pt/ZrO_2 and Pt/CeO_2 catalysts is closely related to their coking resistivity, which has been attributed to the strong interaction of platinum with cationic sites (Zr^{n+} and Ce^{n+}) on the support surface, as shown in the TPR profiles and CO and H_2 chemisorption results. The interfacial sites on Pt-support promote CO_2 dissociation, improving the catalyst stability by shifting the Boudouard reaction [20,35]. Our previous FTIR analysis [20] showed that the Pt-Zr^{n+} interface is active for CO and CO_2 adsorption, with a decrease in the Pt–CO bond strength, inhibiting C–O bond breaking and consequently producing less carbon formation on the catalyst surface. This same kind of interaction could be responsible for the PtCe stability.

4. Conclusions

For partial oxidation of methane, there was no great influence of the nature of the support over the catalytic behavior of Pt-supported catalysts. The composition profiles showed that the partial oxidation reaction proceeds via a two-step mechanism with the total combustion of methane followed by reforming with CO_2 and H_2O produced. The heat released by combustion enhances the reforming reactions. The H_2/CO product ratio varied between 3 and 1.5 over the temperature range of 500–800 °C, with O_2 conversion of 100%.

For reforming of methane with CO_2, the support plays a decisive role on the catalytic stabilities: while PtAl deactivated very fast at 800 °C, owing to the deposition of inactive carbon, the PtZr and PtCe catalysts showed high resistance to coke formation. The H_2/CO ratio is kept lower than 1 because of the occurrence of reverse water–gas shift reaction. The higher stability of the catalysts supported on reducible oxides is closely related to the Pt-support interactions with formation of interfacial sites that promote CO_2 dissociation, inhibiting carbon formation by the Boudouard reaction.

References

[1] J.P. Van Hook, Catal. Rev.—Sci. Eng. 21 (1980) 1.
[2] A.N.J. Van Keulen, M.E.S. Hegarty, J.R.H. Ross and P.F. van den Oosterkamp, Stud. Surf. Sci. Catal. 107 (1997) 537.

[3] L. Pino, V. Recupero, S. Beninati, A.K. Shukla, M.S. Hegde and P. Bera, Appl. Catal. A 225 (2002) 63.
[4] L. Pino, A. Vita, M. Cordaro, V. Recupero and M.S. Hegde, Appl. Catal. A 243 (2003) 135.
[5] D.A. Hickman and L.D. Schmidt, Science 259 (1993) 343.
[6] D.A. Hickman, E.A. Haupfear and L.D. Schmidt, Catal. Lett. 17 (1993) 223.
[7] D.A. Hickman and L.D. Schmidt, J. Catal. 138 (1992) 267.
[8] L.M. Aparicio, J. Catal. 165 (1997) 262.
[9] P.D.F. Vernon, M.L.H. Green, A.K. Cheetham and A.T. Ashcroft, Catal. Today 13 (1992) 417.
[10] A. Erdöhelyi, J. Cserényi and F. Solymosi, J. Catal. 141 (1993) 287.
[11] J.R. Rostrup-Nielsen and J.H. Bak Hansen, J. Catal. 144 (1993) 38.
[12] M.C.J. Bradford and M.A. Vannice, Catal. Rev.—Sci. Eng. 41(1) (1999) 1.
[13] R. Cracium, B. Shereck and R.J. Gorte, Catal. Lett. 51 (1998) 149.
[14] P. Pantu and G.R. Gavalas, Appl. Catal. A 223 (2002) 253.
[15] S.M. Stagg-Wiliams, F.B. Noronha, G. Fendley and D.E. Resasco, J. Catal. 194 (2000) 240.
[16] J.H. Bitter, K. Seshan and J.A. Lercher, J. Catal. 171 (1997) 279.
[17] F.B. Noronha, M. Primet, R. Frety and M. Schmal, Appl. Catal. 78 (1991)125.
[18] H. Lieske, G. Lietz, H. Spindler and J. Völter, J. Catal. 81 (1983) 8.
[19] N. Wagstaff and R. Prins, J. Catal. 59 (1979) 434.
[20] M.M.V.M. Souza, D.A.G. Aranda and M. Schmal, J. Catal. 204 (2001) 498.
[21] A. Trovarelli, Catal. Rev.—Sci. Eng. 38 (1996) 439.
[22] C. Leitenburg, A. Trovarelli and J. Kaspar, J. Catal. 166 (1997) 98.
[23] S. Bernal, J.J. Calvino, G.A. Cifredo, A. Laachir, V. Perrichon and J.M. Hermman, Langmuir 10 (1994) 717.
[24] S. Bernal, J.J. Calvino, M.A. Cauqui, J.M. Gatica, C. Larese, J.A.P. Omil and J.M. Pintado, Catal. Today 50 (1999) 175.
[25] H.C. Yao, M. Sieg and H.K. Plummer Jr., J. Catal. 59 (1979) 365.
[26] D. Dissanayake, M.P. Rosynek, K.C.C. Kharas and J.H. Lunsford, J. Catal. 132 (1991) 117.
[27] F. van Looij, E.R. Stobbe and J.W. Geus, Catal. Lett. 50 (1998) 59.
[28] H.Y. Wang and E. Ruckenstein, Appl. Catal. A 204 (2000) 143.
[29] E. Ruckenstein and H.Y. Wang, J. Catal. 187 (1999) 151.
[30] D. Wolf, M. Barré-Chassonnery, M. Höhenberger, A. Van Veen and M. Baerns, Catal. Today 40 (1998) 147.
[31] M.M.V.M. Souza, D.A.G. Aranda and M. Schmal, Ind. Eng. Chem. Res. 41 (2002) 4681.
[32] A.M. Gadalla and B. Bower, Chem. Eng. Sci. 43 (1988) 3049.
[33] S.C. Tsang, J.B. Claridge and M.L.H. Green, Catal. Today 23 (1995) 3.
[34] J.T. Richardson and S.A. Paripatyadar, Appl. Catal. 61 (1990) 293.
[35] M.C.J. Bradford and M.A. Vannice, J. Catal. 173 (1998) 157.